Iranian Polymer Journal
18 (6), 2009, 501-512

Available online at: http://journal.ippi.ac.ir

Effect of Shell Materials on Microstructure and Properties of Microencapsulated *n*-Octadecane

Changyong Gong, Huanzhi Zhang, and Xiaodong Wang*

Key Laboratory of Beijing City on Preparation and Processing of Novel Polymer Materials, School of Materials Science and Engineering, Beijing University of Chemical Technology, Beijing-100029, PR China

Received 11 February 2009; accepted 23 May 2009

ABSTRACT

Microencapsulated *n*-octadecane phase change materials (PCMs) with polyurethane (PU) and resorcinol-modified poly(melamine-formaldehyde) (PMF) shells were synthesized through interfacial and in-situ polycondensation, respectively, and their microstructures and phase change, thermal stabilities, and anti-osmotic properties were evaluated. FTIR were performed to verify the the quality of encapsulation of *n*-octadecane within two shell materials. Optical phase-contrast microscope and scanning electronic microscopy images indicate a perfect core/shell microstructure and compact polymeric shells of these microcapsules. Differential scanning calorimetry measurements demonstrate the high enthalpies for the melting and crystallization of the microencapsulated *n*-octadecane, while wide-angle X-ray scattering patterns have confirmed that the crystallinity of microencapsulated *n*-octadecane is identical with that of pure *n*-octadecane. Although the two microencapsulated PCMs have good phase change properties, the encapsulation ratio and efficiency of the microcapsules with PU shell are much higher than those of PMF shell. However, the microcapsules with PU shell exhibit good thermal stability but poor anti-osmotic property in comparison with those of PMF shell.

Key Words:

microcapsules;
phase change materials;
n-octadecane;
microstructure;
properties.

INTRODUCTION

Two global issues such as the energy shortage and environmental pollution are becoming more and more serious, especially in the developing countries. Solutions to these problems include improvement of the energy efficiency and the utilization of renewable energy sources. Thermal energy storage is essential for the two solutions. The latent heat storage based on phase change materials (PCMs) is one of the favourable thermal energy storage methods for renewable energy source utilization due to its high-energy storage density and narrow operating temperature range [1]. PCMs have been used as thermal storage and control materials because of the heat absorption and release that occur upon phase change. Although the PCMs are available with a range of transition temperature for varying applications, the PCMs bulk is not easy to handle in practical application because of the super-cooling problem and interfacial combination with the circumstantial materials [2,3]. Microencapsulation is an

(*) To whom correspondence to be addressed.
E-mail: wangxdfox@yahoo.com.cn

important method in various applications to protect specific functional materials, or to release them into the outer phase, within a long period of time. Because microencapsulated PCMs (micro-PCMs) are granular in shape with a core and shell structure, which protect them from being affected by the surrounding environment, they can supply a large heat transfer area so to reduce the reactivity of the PCMs towards the outside environment and control the changes in storage material volume as the phase change occurs [4,5]. Therefore, micro-PCMs have been widely studied for applications in thermal energy fields such as heating and air conditioning of buildings, thermal insulation materials, and thermal adaptable fibres in recent years [6-9].

The design and development of a functional textile with an ability of dynamic heat regulation next to the skin have attracted more and more attention in recent years. Many studies have been carried out on this subject, however, successful applications are limited and still under investigation [10,11]. Therefore, the micro-PCMs have received great interest to improve its thermal insulation to be used in these applications. For the applications of garments and home furnishing products, PCMs should change phases within a temperature range making human feel comfortable, so that they could be utilized for making protective all-season outfits and for abruptly changing climatic conditions [9,12]. The well-known PCMs applied to textiles are linear chain hydrocarbons known as paraffin waxes (or n-alkanes) with a melting temperature (T_m) of 18-36°C, such as heptadecane, hexadecane, octadecane, nonadecane, and eicosane [13]. These PCMs are non-toxic, non-corrosive, chemically inert, easily obtained, and have no unpleasant odour. They have different phase change temperatures, T_m, and crystallization temperature (T_c), depending on the number of carbon atoms in their structures [14,15]. *n*-Octadecane is a desirable PCM for its good ability of thermal storage and release in an appropriate phase change temperature range (23-28°C). Obviously, this phase change temperature is comfortable for human bodies, and its latent heat (241.2 J/g) is higher than that of other PCMs [16,17].

The preparation of micro-PCMs involves enclosing the PCMs in thin and resilient polymer shells to make the PCMs change from solid to liquid and back again within the shells. And thus, the shell materials play an important role in improving the structural anti-permeability, the release controllability, and the thermal stability of the microcapsules. Many studies have demonstrated that poly(melamine-formaldehyde) resin (PMF), urea-formaldehyde resin, and polyurea (PU) are usually selected as the shell materials of the microcapsules for the PCMs protection [18-22]. Khilar et al. reported a kinetic model for describing the dynamics of this microencapsulation [23]. This model was based on diffusion of the hydrophilic monomer through the polymeric shell with an interfacial reaction at the inner surface and could be used to describe the dependence of the microcapsule size on the reaction time as a kinetically controlled process. Fan et al. presented a new method to prevent the micro-PCMs from super-cooling by encapsulating n-octadecane and nucleating agents within the PMF shell [24]. Tamami et al. also reported a new series of polyureas synthesized by the polycondensation of 4-aryl-2,6-bis(4-isocyanatophenyl)pyridines with various aromatic diamines [25].

However, the brittleness of these shell materials is still an obstacle to the industrial application of the micro-PCMs and the studies on the surface modification of these microcapsules are seldom reported at present. In this case, if the microcapsules with tough shell materials could be prepared, the valuable possibility in an essential application may be expected. Moreover, the thermal stability and permeability of the micro-PCMs will also be improved through the modification of the shell materials [26,27]. Therefore, in this study, a series of the micro-PCMs based on the *n*-octadecane core and the modified PMF and PU as shell materials were synthesized by different methods. The aim of this work is to evaluate the properties of two micro-PCMs with different shell materials and to investigate the effects of different shell materials on morphologies, phase change and releasing behaviours of these micro-PCMs.

EXPERIMENTAL

Materials

Melamine with a purity of above 99.5 wt%, formalde-

hyde (37 wt% aqueous solution) and 1,3-benzenediol (resorcinol), 2,4-diisocyanate (TDI) were commercially supplied by Beijing Chemical Reagent Co., China. Amine-terminated polyoxypropylene (Jeffamine T403) was kindly supplied by Yantai Minsheng Chemical Reagent Co., China. *n*-Octadecane with a purity of 90 wt% was purchased from Tianjin Alfa Aesar Co., China. Sodium salt of styrene-maleic anhydride copolymer (SMA) used as emulsifier was kindly supplied by Shanghai Leather Chemical Company. Ammonium chloride as a nucleating agent and acetone as an extracting solvent were also obtained from Beijing Chemical Reagent Co., China.

Synthesis of Microcapsules

The microencapsulated *n*-octadecane with resorcinol-modified PMF shell was synthesized by in-situ polymerization. The procedure consisted of the synthesis of pre-polymer solution, the preparation of emulsion, and the formation of shell material. The pre-polymer solution was prepared by mixing melamine, formaldehyde, and distilled water in a round flask. *n*-Octadecane, SMA, 5 wt% resorcinol, and distilled water were emulsified mechanically at 50°C with a stirring rate of 8000 rpm for 2 h. Resorcinol was added to achieve little cross-linking with the melamine-formaldehyde prepolymer. The prepolymer solution was added dropwise into the emulsion while the emulsion was stirred at a rate of 600 rpm. After the complete addition of the prepolymer, 5 wt% ammonium chloride was added into the solution and it was continuously stirred at 60°C for 90 min. The pH of the emulsion was adjusted to 9.0 with 10 wt% triethanolamine solution, which terminated the reaction. Then, the resultant microcapsules were filtered and washed with 30 wt% ethanol aqueous solution. The wet powders were dried in a vacuum oven to remove the water.

The microencapsulated *n*-octadecane with modified PU shell was synthesized through interfacial polycondensation. An oil solution was prepared by mixing TDI, *n*-octadecane, and acetone in a round-bottom flask with stirring for several minutes. An oil-in-water (O/W) emulsion was formed by pouring the oil solution dropwise into an aqueous solution with 5 wt% SMA as an emulsifier. Amine-terminated polyoxypropylene was dissolved in an aqueous solution containing 0.1 wt% SMA. Subsequently, the amine-terminated polyoxypropylene aqueous solution was added into the emulsion with a stirring rate of 600 rpm. After the addition of all the aqueous amine-terminated polyoxypropylene, the solution was continuously stirred at 60°C for 3 h. The resultant microcapsules were filtered and washed with 30 wt% aqueous ethanol solution at approximately 50°C. The wet powders were dried in a vacuum oven to remove the water.

Characterization

Fourier transform infrared (FTIR) spectra of the samples were obtained by using a Bruker Tensor-27 FTIR spectrophotometer. An Olympus BX50 optical phase-contrast microscope was employed to investigate the structure of the microcapsules. Morphologies were obtained by using a Hitachi S-4700 scanning electron microscope (SEM). The microcapsules size distribution was performed by light diffraction using a LA-920 laser particle-size analyzer and the mean diameters of the microcapsules were determined. Wide angle X-ray scattering (WAXS) measurement was carried out by a Rigaku D/max-r C diffractometer (40 kV, 50 mA) with Cu-K_α radiation ($\lambda = 0.154$ nm) with a scanning rate of 5°/min. Differential scanning calorimetry (DSC) was performed by using a TA Instruments Q100 differential scanning calorimeter and all measurements were carried out under N_2 atmosphere at a heating or cooling rate of 10°C/min of each sample with about 10 mg weight. The first heating scan was carried out from -20 to 50°C and the sample was held at this temperature for 5 min to diminish the thermal and processing history before the formal measurements.

Thermogravimetric analysis (TGA) for the microcapsules was carried out at a heating rate of 10°C/min under nitrogen gas atmosphere by using a TA Instruments Q50 TGA thermal analyzer. Anti-osmosis measurement was performed by a 723PC spectrophotometer. The releasing rate (weight percentage of the released substance) of the microencapsulated *n*-octadecane was measured by dispersing 10 g microcapsules in 50 mL acetone as an extraction solvent with a slight stirring rate of 200 rpm and the data was conversed through the transmittance of spectrophotometer.

RESULTS AND DISCUSSION

Microstructure

The synthesis of two types of the microencapsulated *n*-octadecane is performed by in-situ or interfacial polycondensation with the microcapsule shells fabricated on the surface of the *n*-octadecane droplets by polycondensation of the reactive monomers. The chemical structures of these two types of microcapsules were confirmed by FTIR spectra as presented in Figure 1. In the spectrum of the microencapsulated *n*-octadecane with resorcinol-modified PMF shell, one can see a broad absorption band around 3350 cm^{-1} corresponding to the hydroxyl, imino, and amino stretching vibrations. The alkyl C–H and C–N multiple stretching vibrations in the triazine ring are found around 2950 cm^{-1} and 1555 cm^{-1}, respectively. The C–H bending vibrations in methylene group appear at 1490 cm^{-1} and 1360 cm^{-1} due to methylene bridges [8]. The characteristic absorption bands for the aliphatic C–N vibration appear between 1200 and 1170 cm^{-1}, while the characteristic triazine ring bending vibration is observed at 810 cm^{-1}. Meanwhile, the broad peak at around 3390 cm^{-1}, which is overlapped by the imino and amino stretching peaks, also corresponds to the phenolic hydroxyl stretching vibration. The peaks at around 1510 cm^{-1} and 1160 cm^{-1} show the phenyl ring and the C–O stretching vibrations in the phenyl ring, respectively [28]. The presence of the phenyl ring and phenolic hydroxyl indicates that resorcinol has been linked into the melamine-formaldehyde copolymer chains. These assignments indicate that the resorcinol-modified PMF shell has been formed which implies that the *n*-octadecane is successfully encapsulated by the resorcinol-modified PMF. It was also confirmed in our pervious work [29]. On the other hand, the spectrum of the microencapsulated *n*-octadecane with PU shell demonstrates a series of strong absorption bands corresponding to the hydrogen-bonded N–H stretching vibration at 3300~3360 cm^{-1} and 1539 cm^{-1} [30]. The C–H stretching vibrations of aliphatic amines are also observed at 2950 cm^{-1} and 2850 cm^{-1}, respectively. The peak for –N=C=O in diisocyanates at 2270 cm^{-1} disappears due to the reaction of TDI with the amine-terminated polyoxypropylene, and a band assigned to the hydrogen bonding with urea carbonyl stretching appears at 1655 cm^{-1}. The characteristics bands of PU at 1592, 1409, 1109 and 820 cm^{-1} may be assigned to the C=C, C–C, and C–O stretching vibrations and C–H bending vibration in aromatic groups, respectively [17]. It can be concluded from these characteristic peaks that the PU shell of the microcapsules is successfully formed. The FTIR spectrum of *n*-octadecane is also displayed as a reference in Figure 1. All the characteristic peaks for *n*-octa-decane can be clearly distinguished in the spectra of these two microcapsules, which verify that *n*-octa-decane has been successfully encapsulated by the corresponding copolymers.

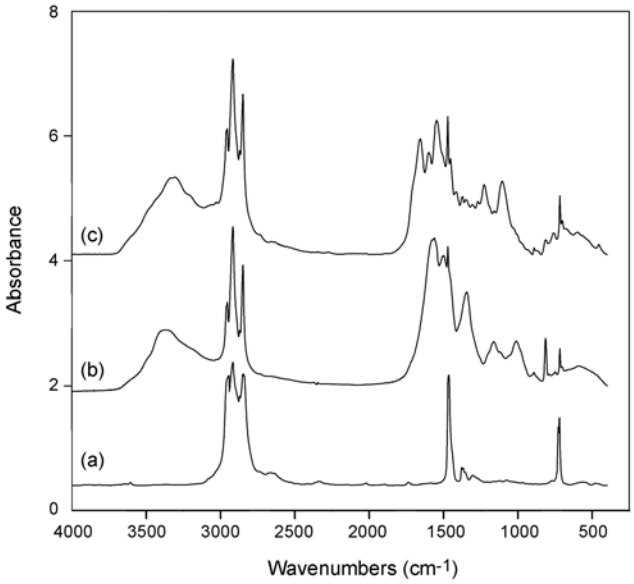

Figure 1. FTIR spectra of: (a) pure *n*-octadecane, (b) microcapsules with PMF shell, and (c) microcapsules with PU shell.

The microencapsulated *n*-octadecane with the PMF and PU shells were firstly observed by an optical phase-contrast microscope, and their digital photos are shown in Figures 2a and 2b, respectively, which demonstrate that these microcapsules are regular spheres without any obvious disfigurement on their surfaces. It is notable that both of the microcapsules reveal a legible core-shell microstructure, where a white-colour circle corresponding to the shell surrounds a dark-colour core which is the encapsulated *n*-octadecane, can be clearly distinguished. It can also be found that the PMF shell material of the microencapsulated *n*-octadecane shows a higher brightness than the PU shell, which indicates that the

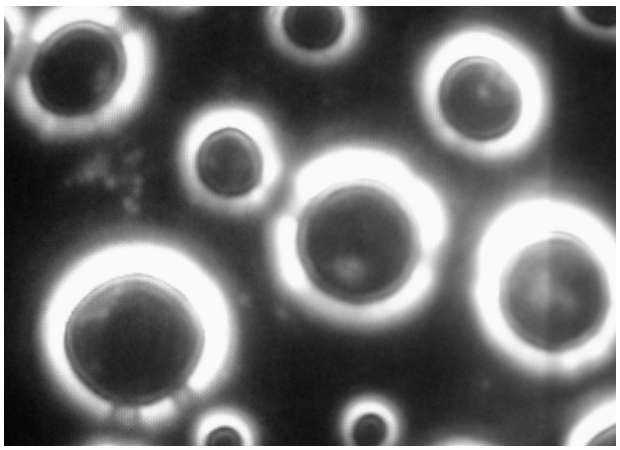

(a)

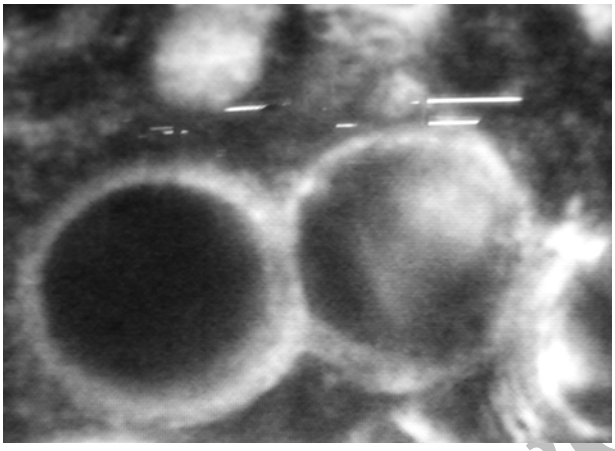

(b)

Figure 2. Optical phase-contrast microscope images of: (a) microcapsules with PMF shell and (b) microcapsules with PU shell.

latter has much higher cross-linking density. The morphological structures of the microencapsulated *n*-octadecane are also investigated by SEM images, as shown in Figures 3a-3c. The two types of the microcapsules present a spherical shape with a compact surface, where no disfigurement is found, and their typical core-shell inner microstructure can also be confirmed by the SEM image of a broken microcapsule as shown in Figure 3c. However, the microcapsules with the PU shell display a smoother surface than those with the PMF shell. This result is attributed to their different polymerization mechanisms. Although the two microcapsules initiated with the formation of micelles containing the core droplets of *n*-octadecane in aqueous solution through emulsification, the

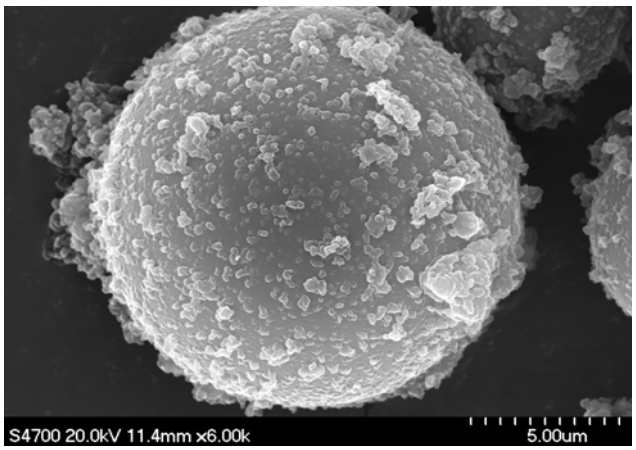

(a)

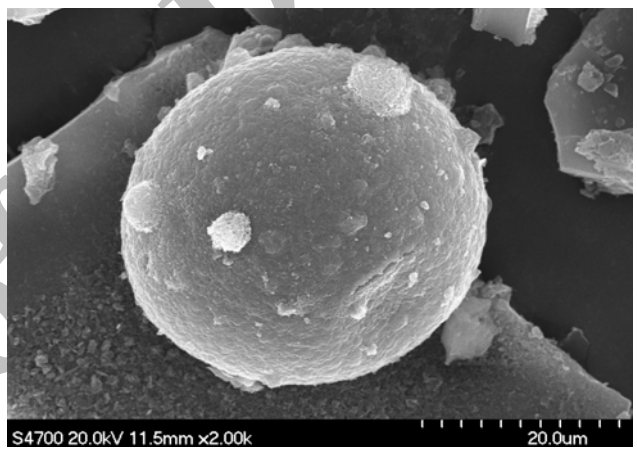

(b)

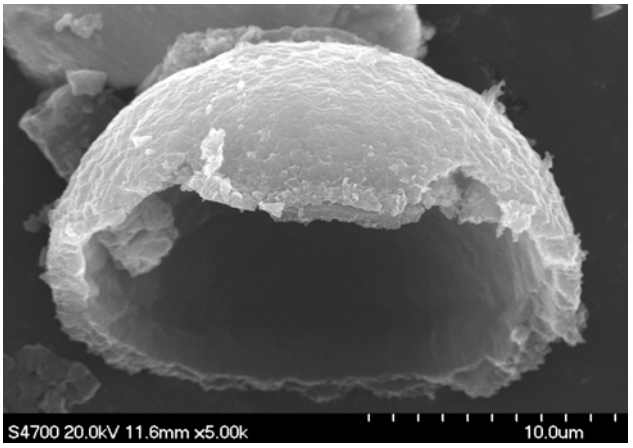

(c)

Figure 3. SEM images of: (a) microcapsules with PMF shell and (b and c) microcapsules with PU shell.

followed polycondensation mechanisms were different. During the synthesis process of the

microencapsulated *n*-octadecane with the resorcinol-modified PMF shell as was described in our previous work [29], the hydrophilic groups of the emulsifier alternatively arrange along its hydrophobic chains, thus associated with water molecules and trimly cover the surface of *n*-octadecane oil droplets with hydrophobic chains oriented into the oil droplets and hydrophilic groups out of the oil droplets. Positively charged melamine-formaldehyde prepolymers were attracted by anionic carboxyl groups produced through the hydrolysis of the hydrophilic groups in the anionic emulsifier chains. Then, the in-situ polycondensation between the melamine-formaldehyde prepolymers occurs on the surface of the droplets of *n*-octadecane to form the PMF shells. Owing to the non-uniform distribution of the melamine-formaldehyde prepolymers on the surface of the oil droplets, the formed shell was coarse. However, for the synthesis of the microencapsulated *n*-octadecane with the PU shell, the micelles consisting of *n*-octadecane and TDI was formed in an aqueous emulsion. Subsequently, another requisite monomer, amine-terminated polyoxypropylene, is dropped into the emulsion to react with TDI and forms the PU shell. This interfacial polymerization is tardy, thus the surface of the shell is smooth. The mean particle diameters of the microcapsules were determined by the laser particle-size analyzer as listed in Table 1. In this study, the samples with two different core/shell material weight ratios were prepared for each type of the microencapsulated *n*-octadecane. It can be found that the mean particle size of the microcapsules with the PU shell is slightly larger than that of PMF shell, and furthermore, the microcapsules with a high core/shell weight ratio have a large mean particle size.

Crystallography of Microencapsulated *n*-Octadecane

Figure 4 shows the WAXS patterns of pure *n*-octadecane and the microencapsulated *n*-octadecanes with different shell materials, indicating the crystallinity of the *n*-octadecane encapsulated within the two different polymeric shells. In the pattern of pure *n*-octadecane, four well-resolved diffraction peaks at 2θ of 19.20º, 19.71º, 23.28º, and 24.60º can be observed, and they can be indexed as (011), (012), (101) and (102) reflections of the α-crystal phase of *n*-octadecane segments, respectively. In addition, the reflection at 2θ of 7.61, 42.30, and 44.42º corresponds to the plane (003), (215), and (205) of the β-crystal, respectively [31]. These results indicate that the crystal of *n*-octadecane is triclinic [32,33]. As the PMF and PU shells are amorphous, the reflections appearing in the patterns of all the microencapsulated

Table 1. Phase change properties and thermal stabilities of pure *n*-octadecane and the microcapsules with different shell materials.

Sample code	Core/shell ratio (wt/wt)	Mean particle diameter (μm)	T_m (ºC)	ΔH_m (J/g)	T_c (ºC)		ΔH_c (J/g)	Encap. ratio (wt%)	Encap. efficiency (%)	Temperature at characteristic weight loss (ºC)		Temperature at rapid weight loss (ºC)	Char yield at 550ºC (wt%)
					α	β				2 (wt%)	10 (wt%)		
1	100/0	–	26.4	214.6	24.6	22.5	216.2	–	–	–	–	–	–
2	70/30 (PU)	15.8	27.0	188.9	22.6	21.3	187.9	88.0	87.4	60.6	138.6	161.3	12.4
3	75/25 (PU)	17.6	26.8	171.8	22.8	21.6	171.3	80.1	79.6	48.3	135.0	160.7	8.0
4	70/30 (PMF)	13.9	27.1	135.2	22.6	19.7	136.3	63.0	90.0	139.3	172.0	217.3	0.6
5	75/25 (PMF)	14.8	26.9	146.5	23.1	21.4	149.2	68.3	92.0	122.3	160.5	200.7	0.8

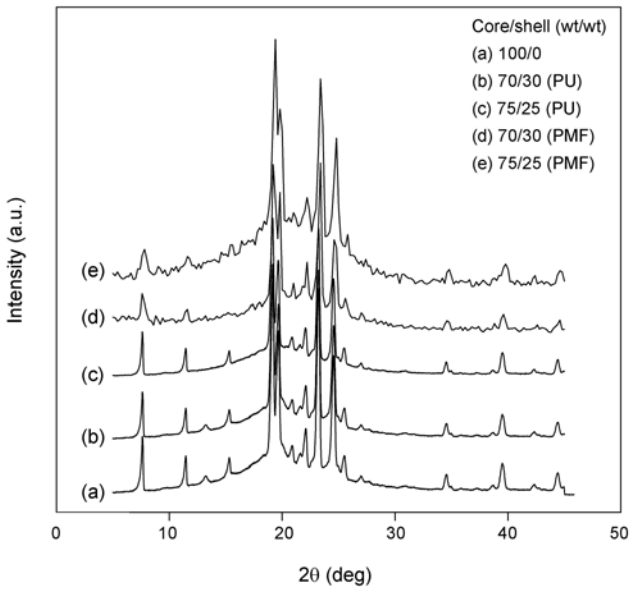

Figure 4. WAXS patterns of the pure and microencapsulated *n*-octadecane with different shells.

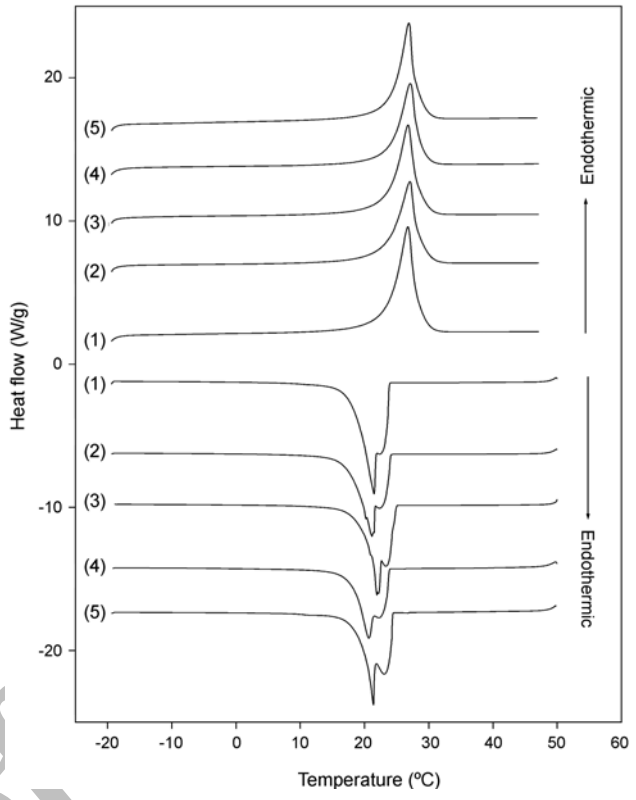

Figure 5. DSC thermograms of pure and microencapsulated *n*-octadecane with different shells (The numbers of the thermograms correspond to the sample codes in Table 1).

n-octadecane should be assigned to the *n*-octadecane encapsulated within the microcapsules. It is noticed that WAXS patterns of these microencapsulated *n*-octadecane are similar to those of the pure *n*-octadecane, and there is little difference between the patterns of the microcapsules with PU and PMF shells. These results indicate that the crystal system of the *n*-octadecane encapsulated within the microcapsules is the same as that of pure *n*-octadecane. An evaluation of the mean particle size of the two types of microcapsules demonstrated that *n*-octadecane was encapsulated within a spherical room with an average diameter of 14-16 μm. The crystal configuration implies that, in the case of particle size, the two microcapsules provide enough space for the motion of *n*-octadecane chains, and the crystallization of the *n*-octadecane within microcapsules does not exhibit any confined behaviour. It is concluded that the *n*-octadecane encapsulated within the two shell materials can perform a phase change behaviour.

Phase Change Behaviour

The phase change enthalpies and phase change temperatures of pure and the microencapsulated *n*-octadecane with different shell materials were measured by DSC, and the heating and cooling thermograms are shown in Figure 5. The melting and crystallization parameters of all the samples obtained from DSC analysis are listed in Table 1. It is observed that a single peak appears on the DSC thermogram for each sample, whereas its shoulder of the peak becomes wider when *n*-octadecane is encapsulated within the microcapsules. This phenomenon indicates that the phase-changeable temperature range of the microencapsulated *n*-octadecane is extended. The melting peak temperatures of all the microcapsules are higher than that of *n*-octadecane, which may be attributed to low thermal conductivity of the shell materials. As it was discussed in our previous study [29], the thermal conductivity of the shell materials affects the heat transfer rate from the outside to the PCM inside the shells, which in turn affects the phase change temperatures of the microcapsules. In addition, it is also found that the microcapsules with low core/shell weight ratios have higher melting peak temperatures in comparison with microcapsules having higher core/shell weight ratios. This finding is attributed to the poor thermal conductivity caused by

their thick shells as well as the crystals of *n*-octadecane formed by the heterogeneous nucleation of the inner wall, which can lead to a higher melting temperature.

However, it is observed that two peaks appear on the cooling thermograms for both the pure and the microencapsulated *n*-octadecane, corresponding to two crystallization temperatures of *n*-octadecane (i.e., its α- and β-crystal phases) [8]. It is evident that α-peak is enhanced when *n*-octadecane is encapsulated. During crystallization of the microencapsulated *n*-octadecane, α-peak is attributed to the heterogeneously nucleated liquid-rotator transition, which may be due to the crystallization of *n*-octadecane on the inner wall of the microcapsules, and β-peak is attributed to the homogeneously nucleated liquid-crystal transition [34]. These crystalline bulk phases emerge in-between one another and exhibit a very wide temperature region during the melting process; therefore there is only one single melting peak in the DSC heating thermogram (Figure 5). In addition, it is also noted that the α-peak appearing on the DSC cooling thermogram of pure *n*-octadecane is slender compared to that of the microencapsulated *n*-octadecane. This can be attributed to the heterogeneous nucleation caused by the impurity of *n*-octadecane [29].

It is also observed that there is a declined crystallization peak temperatures of the microencapsulated *n*-octadecane in comparison with that of pure *n*-octadecane, which is attributed to the crystallization behaviour confined to the inner space of the microcapsules as well as the poor thermal conductivity of shell materials. The microcapsules with the PMF shell at a core/shell weight ratio of 70/30 exhibit the most significant confined crystallization behaviour due to their smallest mean particle size among the four samples, and thus the largest decrements in the T_cs (α and β) were obtained. In the opposite, the microcapsules with the PU shell at a core/shell weight ratio of 75/25 have a large particle size of around 16 μm therefore, the confinement of crystallization is not remarkable. The melting and crystallization behaviours of the microencapsulated *n*-octadecane are affected not only by the mean particles, but also by the shell materials. As it is evident in Table 1, pure *n*-octadecane has a high latent heat of fusion (ΔH_m) of 214.6 J/g and a high enthalpy of crystallization (ΔH_c) of 216.2 J/g. The phase change enthalpies of all microcapsules, which are normalized to the amount of *n*-octadecane in terms of the core/shell weight ratios, are lower than that of pure *n*-octadecane. It is noteworthy that both T_ms and T_cs of the microcapsules with PU shell are closer to pure *n*-octadecane, while the two corresponding parameters of the samples with PMF shell decline remarkably. These results indicate that PU can encapsulate *n*-octadecane more efficiently during the interfacial polycondensation than the PMF in in-situ polycondensation, and thus, preserves the phase change properties of the core material much better than the PMF shell. This is an indication that the encapsulation efficiency of PMF shell materials is lower than that of PU materials during the synthesis of the microencapsulated *n*-octadecane.

Encapsulation Ratio and Efficiency

Encapsulation ratio and efficiency, as two important parameters, are used to describe the phase change properties of microencapsulated *n*-octadecane, which were determined by analysis of the DSC thermograms. The enthalpies of the microencapsulated *n*-octadecane from solid-liquid phase change strongly depend on the encapsulation ratio and efficiency of the microencapsulated *n*-octadecane, which affects the efficiency of the micro-PCMs. The encapsulation ratios can be calculated by eqn (1) on the basis of the fusion heat obtained from the DSC analysis:

$$R(\%) = \frac{\Delta H_{m,Micro-PCMs}}{\Delta H_{m,PCM}} \times 100 \qquad (1)$$

where,

$\Delta H_{m,Micro\text{-}PCMs}$: Latent heat of fusion of the microencapsulated *n*-octadecane;

$\Delta H_{m,PCM}$: Latent heat of fusion of pure *n*-octa-decane;

R : Encapsulation ratio

The results are summarized in Table 1. Whereas, the encapsulation ratio represents the exact weight percentage of the core material in the microcapsules, while the core/shell weight ratio is considered as the dry weight ratio of the feed raw materials. It is found that, because the interfacial polycondensation

between TDI and amine-terminated polyoxypropylene was not performed completely, the encapsulation ratio was always higher than the value derived from the core/shell weight ratio. However, the fabrication of PMF onto the surface of the *n*-octadecane droplets was partially failed, resulting in a lower encapsulation ratio than the core/shell weight ratio. Evidently, the encapsulation ability is poor for the in-situ polycondensation due to its mechanism and weak ability for the melamine-formaldehyde prepolymers to integrate into the polymer shells. In the case of interfacial polycondensation, the encapsulation ratio is more suitable to evaluate the efficiency of the microencapsulated *n*-octadecane. Furthermore, the encapsulation efficiency can be calculated by the phase change enthalpies obtained from the DSC thermograms according to the following equation:

$$E = \frac{\Delta H_{m,Micro-PCMs} + \Delta H_{c,Micro-PCMs}}{\Delta H_{m,PCM} + \Delta H_{c,PCM}} \quad (2)$$

where,

$\Delta H_{c,Micro\text{-}PCMs}$: Enthalpy of the microencapsulated *n*-octadecane crystallization;

$\Delta H_{c,PCM}$: Enthalpy of pure *n*-octadecane crystallization;

E : Encapsulation efficiency.

For the microencapsulated *n*-octadecane with the PU shell at a core/shell weight ratio of 70/30, the encapsulation efficiency of *n*-octadecane is only 87.4%. While the core/shell weight ratio increases to 75/25, the encapsulation efficiency declines to 79.6%.

Owing to the increase of the core/shell ratio, the shell becomes thin and fragile, and the core material can leak out from the microcapsules easily, resulting in the low encapsulation efficiency. However, it can be noticed that the microcapsules with the PMF shell have much lower encapsulation efficiency than those with the PU shell, which is attributed to the fragile shell material based on PMF. It is clear that PMF is more brittle than PU, and it breaks more easily. Thus, the low encapsulation efficiency is mainly attributed to the leakage of *n*-octadecane from the broken microcapsules. It is also deduced from the above results that the optimal core/shell weight ratio is 70/30 for the synthesis of the microcapsules with PU shell, while the core/shell weight ratio of 75/25 is the optimal value for a PMF shell.

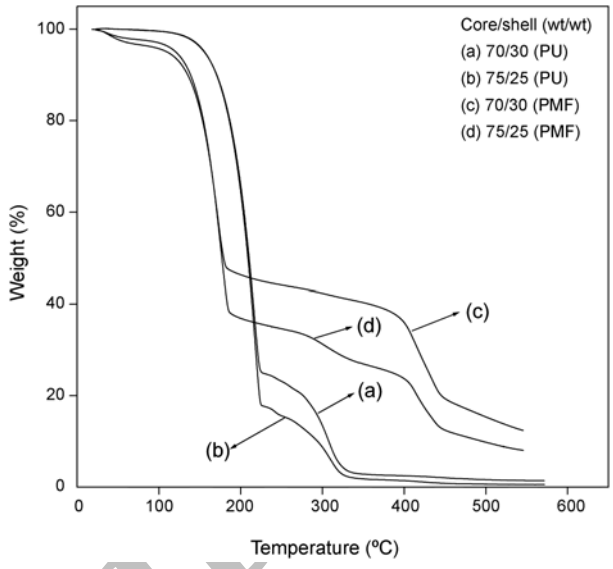

Figure 6. TGA thermograms of microcapsules with different shells.

Thermal Stabilities

Effects of the shell materials on the thermal stabilities of the microcapsules are also investigated by means of TGA technique. Figure 6 shows the TGA thermograms presenting the sample mass loss as a function of the temperature, and the obtained data are also summarized in Table 1. The thermal decomposition of all the samples takes place in the programmed temperature range of 25-550°C which occurs through a two-step degradation pattern. The weight loss starting at about 95ºC and 130°C at the first stage corresponds to the softening and cracking of the PMF and PU shells, respectively, followed by the leaking out of *n*-octadecane from the microcapsules. After removing the whole *n*-octadecane from the microcapsules, the shell materials begin to decompose at the second stage of weight loss. It is notable that the weight losses of all the microcapsules with the PMF shell occur at much lower temperatures than those of the PU shell either at the first or the second stages, which can be concluded that the stability of the PMF material is poor. In addition, the microcapsules with low weight ratios of the core/shell materials exhibit better thermal stabilities compared to high core/shell weight ratios, and thus result in high char yields.

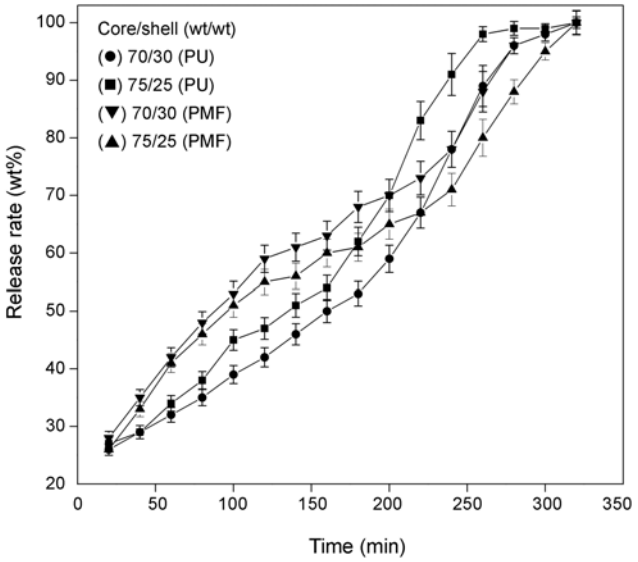

Figure 7. Release curves of microcapsules with different shells.

Anti-osmosis

The anti-osmosis is an important parameter representing the durability during the use of the microcapsules, and determines the application prospect of the micro-PCMs. The high cross-linking between the macromolecules can lead to a tight chain structure, and thus a highly compact material is achieved by anti-osmosis technique. However, a weak tightness of the shell materials can make the core materials diffuse easily through the shell layers, which results in poor durable microcapsules. The reason is that the shell is not closely knit and there are lacunas or capillaries in the shell, resulting in high release rates. On the contrary, the smooth and orbicular shell with high toughness can increase the tightness, and thus can decrease the release rates of the core materials. As a result, the anti-osmosis is enhanced. The tightness of the shell materials is affected by the chemical structures as well as the higher mass ratio of core and shell. Anti-osmosis test measured by the weight loss of the extracted microcapsules (i.e., releasing rate of *n*-octadecane from the microcapsules) can be used to evaluate the sealing performance of the PU and PMF shells, and thus estimate the durability of the microcapsules prepared in this study.

Figure 7 presents the releasing rates of the microencapsulated *n*-octadecane with PU and PMF shells as the function of the storage time, which indicates a significant influence of the shell materials on the anti-osmosis test. The microencapsulated *n*-octadecane with PMF shell has a higher releasing rate than with PU shell. It is understandable that the polyurea shell containing long alkyl segments has a tight structure, resulting in low permeability. However, when the releasing time elapses over about 200 min, the microcapsules with PU shell exhibit a very high releasing rate. This can be attributed to the low cross-linking of the PU shell, which may result in poor durability. In addition, it is also found that the weight ratio of the core/shell materials demonstrates a significant influence on the release behaviours of the microcapsules.

As can be seen in Figure 7, it is clearly suggested that the release rate of the microcapsules increases with increase in the weight percentage of the core materials. The reason is that the shell of the microcapsules with high core/shell weight ratio is very thin. Therefore, the core material releases fast from the microcapsules, which results in a high releasing rate.

In summary, the two types of the microencapsulated *n*-octadecane were synthesized on the basis of the shell material modification to achieve better properties than the conventional systems. As it is expected, these microcapsules have high physical strength and toughness to bear certain pressure or an impact load, which leads to a certain solution to the crack and leakage problems of core materials through the well-organized synthesis and some available protective materials. These microcapsules also exhibit satisfactory performances in thermal stability and structural durability for further industrial applications. Furthermore, these two types of microencapsulated *n*-octadecane have potential applications in diverse areas, such as building heating/cooling systems, thermo-regulated fibers, fabrics, coatings, foams, home furnishing products and building materials, which make solar energy or large amounts of other excess heat to be utilized effectively.

CONCLUSION

The microencapsulated *n*-octadecane with the modified PMF and PU shells were prepared through in-situ and interfacial polycondensation, respectively. The optical phase-contrast microscope and FTIR spectra

confirmed that *n*-octadecane was successfully encapsulated within the shells of the two materials, while the SEM images indicated that these microcapsules have a perfect core/shell microstructure and compact polymeric shell. Although the two types of the microencapsulated *n*-octadecane have good phase change properties, the encapsulation ratio and encapsulation efficiency of the microcapsules with PU shell are much higher than the case of PMF shell. However, the microcapsules obtained with PU shell also exhibit a good thermal stability, though poor anti-osmotic property in comparison with those having PMF shell.

REFERENCES

1. Farid MM, Khudhair AM, Razack SAK, Al-Hallaj S, A review on phase change energy storage: materials and applications, *Energy Convers Manag*, **45**, 1597-1615, 2004.
2. Leitch P, Tassinari TH, New materials in the new millennium, *J Ind Text*, **29**, 173-191, 2000.
3. R. Yang, H. Xu, Y.P. Zhang, Preparation, physical property and thermal physical property of phase change microcapsule slurry and phase change emulsion, *Sol Energy Mater Sol Cells*, **80**, 405-416, 2003.
4. Tzvetkvo G, Fink RH, Temperature-dependent X-ray microspectroscopy of phase change core-shell microcapsules, *Scripta Mater*, **59**, 348-351, 2008.
5. You M, Zhang XX, Li W, Wang XC, Effects of Micro-PCMs on the fabrication of MicroPCMs/polyurethane composite foams, *Thermochim Acta*, **472**, 20-24, 2008.
6. Khudhair AM, Farid MM, A review on energy conservation in building applications with thermal storage by latent heat using phase change materials, *Energy Conversion Manag*, **45**, 263-275, 2004.
7. Suryanarayana C, Rao KC, Kumar D, Preparation and characterization of microcapsules containing linseed oil and its use in self-healing coatings, *Prog Org Coat*, **63**, 72-78, 2008.
8. Zhang XX, Fan YF, Tao XM, Yick KL, Fabrication and properties of microcapsules and nanocapsules containing *n*-octadecane, *Mater Chem Phys*, **88**, 300-307, 2004.
9. Mulligan JC, Colvin DP, Microencapsulated phase change material suspensions for heat transfer in spacecraft thermal systems, *J Spacecraft Rockets*, **33**, 278-284, 1996.
10. Shin Y, Yoo D, Son K, Development of thermoregulating textile materials with microencapsulated phase change materials (PCM). IV: performance properties and hand of fabrics treated with PCM microcapsules, *J Appl Polym Sci*, **97**, 910-915, 2005.
11. Shin Y, Yoo D, Son K, Development of thermoregulating textile materials with microencapsulated phase change materials (PCM) IV. Performance properties and hand of fabrics treated with PCM microcapsules, *J Appl Polym Sci*, **97**, 910-915, 2005.
12. Cho JS, Kwon A, Cho CG, Microencapsulation of octadecane as a phase change material by interfacial polymerization in an emulsion system, *Colloid Polym Sci*, **280**, 260-266, 2002.
13. Liu X, Liu HY, Wang SH, Zhang L, Cheng H, Preparation and thermal properties of form-stable paraffin phase change material encapsulation, *Sol Energy*, **80**, 1561-1567, 2006.
14. Mark E, Use of microencapsulated phase change materials to ehhance the thermal performance of apparel, *Am Soc Mech Eng*, **44**, 235-239, 1999.
15. Su JF, Wang LX, Ren L, Preparation and mechanical properties of thermal energy storage microcapsules, *Colloid Polym Sci*, **284**, 224-228, 2005.
16. Su JF, Wang LX, Ren L, Fabrication and thermal properties of microPCMs: used melamine formaldehyde resins as shell material, *J Appl Polym Sci*, **101**, 1522-1528, 2006.
17. Su JF, Wang LX, Ren L, Synthesis of polyurethane microPCMs containing *n*-octadecane by interfacial polycondensation: influence of styrene-maleic anhydride as a surfactant, *Colloid Surf A: Physicochem Eng Asp*, **299**, 268-275, 2007.
18. Frere W, Danicher L, Gramain P, Preparation of polyurethane microcapsules by interfacial polycondensation, *Eur Polym J*, **34**, 193-199, 1998.
19. Kim EY, Kim HD, Preparation and properties of microencapsulated octadecane with waterborne

polyurethane, *J Appl Polym Sci*, **96**, 1596-1604, 2005.
20. Zhang XX, Fan YF, Tao XM, Yick KL, Crystallization and prevention of supercooling of microencapsulated *n*-alkanes, *J Colloid Interface Sci*, **281**, 299-306, 2005.
21. Li W, Zhang XX, Wang XC, Niu JJ, Preparation and characterization of microencapsulated phase change material with low remnant formaldehyde content, *Mater Chem Phys*, **106**, 437-442, 2007.
22. Fan YF, Zhang XX, Wu CZ, Wang XC, Thermal stability and permeability of microencapsulated *n*-octadecane and cyclohexane, *Thermochim Acta*, **429**, 25-29, 2005.
23. Yadav SK, Suresh AK, Khilar KC, Microencapsulation in polyurea shell by interfacial polycondensation, *AIChE J*, **36**, 431-438, 1990.
24. Fan YF, Zhang XX, Wang XC, Li J, Zhu QB, Super-cooling prevention of microencapsulated phase change material, *Thermochim Acta*, **413**, 1-6, 2004.
25. Tamami B, Koohmareh GA, Synthesis and characterization of polyureas derived from 4-aryl-2,6-bis(4-isocyanatophenyl)pyridines, *Des Monomers Polym*, **10**, 221-233, 2007.
26. Sarier N, Onder E, The manufacture of microencapsulated phase change materials suitable for the design of thermally enhanced fabrics, *Thermochim Acta*, **452**, 149-160, 2007.
27. Sun G, Zhang Z, Mechanical strength of microcapsules made of different wall materials, *Int J Pharm*, **242**, 307-311, 2002.
28. Zhang XX, Mao XM, Yick KL, Fan YF, Expansion space and thermal stability of microencapsulated *n*-octadecane, *J Appl Polym Sci*, **97**, 390-396, 2005.
29. Zhang H, Wang X, Fabrication and performances of microencapsulated phase change materials based on *n*-octadecane core and resorcinol-modified melamine-formaldehyde shell, *Colloid Surf A: Physicochem Eng Asp*, **332**, 129-138, 2009.
30. Hong K, Park S, Preparation of polyurethane microcapsules with different soft segments and their characteristics, *React Funct Polym*, **42**, 193-200, 1999.
31. Kraack H, Sirota EB, M. Deutsch, Measurements of homogeneous nucleation in normal-alkanes, *J Chem Phys*, **112**, 6873-6885, 2000.
32. Chazhengina SY, Kotelnikova EN, Filippova IV, Filatov SK, Phase transitions of *n*-alkanes as rotator crystals, *J Mol Struct*, **647**, 243-257, 2003.
33. Sirota, EB. Herhold AB, Transient phase-induced nucleation, *Science*, **283**, 529-532, 1999.
34. Oliver MJ, Calvert PD, Homogeneous nucleation of *n*-alkanes measured by differential scanning calorimetry, *J Cryst Growth*, **30**, 343-351, 1975.